CrossMark

Revisiting the dissolution of biogenic Si in marine sediments: a key term in the ocean Si budget

Patrick Frings[1,2]

Abstract Of the $\sim 240 \times 10^{12}$ mol year^{-1} of biogenic silica (bSi) produced by diatoms and other silicifying organisms, only roughly 3%–4% escapes dissolution to be permanently buried. At the global scale, how, where and why bSi is preserved in sediment is not well understood. To help address this, I compile 6245 porewater dissolved Si concentrations from 453 sediment cores, to derive the concentration gradient at the sediment–water interface and thus diffusive fluxes out of the sediment. These range from <0.002 to 3.4 mol m^{-2} year^{-1}, and are independent of temperature, depth and latitude. When classified by sediment lithology, predominantly siliceous sediments unsurprisingly have higher mean diffusive fluxes than predominantly calcareous or clay-rich sediment. Combined with the areal extent of these lithologies, the 'best-guess' global sedimentary bSi recycling flux is 69×10^{12} mol year^{-1}.

Keywords Biogenic silica · Diatoms · Ocean Si cycle · Dissolution

✉ Patrick Frings
  patrick.frings@gfz-potsdam.de

1   Department of Geoscience, Swedish Museum of Natural History, 10405 Stockholm, Sweden

2   Earth Surface Geochemistry, GFZ German Research Centre for Geosciences, 14473 Telegrafenberg, Potsdam, Germany

1 Introduction

Ocean dissolved Si concentrations (hereafter [Si]) span two orders of magnitude, from <1 μmol L^{-1} in surface gyres to almost 200 μmol L^{-1} in parts of the deep ocean. Yet even these regions are highly undersaturated—amorphous Si solubility is ca. 1800 μmol L^{-1} at 20 °C (Gunnarsson and Arnórsson 2000). The ubiquitously high degree of undersaturation attests to the efficiency with which biosilicifying organisms, in particular the diatoms, can take dissolved Si and precipitate it in their biogenic silica (bSi) skeletons. This high degree of undersaturation also means that much of the bSi produced dissolves after the organism's death. Dissolution begins in the euphotic zone, and continues throughout the water column and into the upper sediment, until the bSi is exhausted (leading to large parts of the ocean floor devoid of siliceous remains) or the bSi reaches equilibrium with sediment porewaters and dissolution ceases.

The canonical figure for annual bSi production is 240 Tmol (Tréguer and De La Rocha 2013), approximately 25× annual inputs of Si to the ocean (Frings et al. 2016). Various approaches consistently indicate a large fraction—around 50%–60%—is remineralised in the upper 100 m. This leaves around 100 Tmol year^{-1} bSi as export production (Tréguer and De La Rocha 2013). The fate of this bSi is less well understood, though ca. 10 Tmol year^{-1} must be preserved to balance the inputs at steady-state. In particular, the relative fractions of dissolution occurring in the water column and in the sediments are not well constrained, but has implications for how we quantify the past and present Si cycle. Diffusive fluxes of Si across the sediment–water interface can be used to estimate bSi dissolution in the sediment; previous global scale estimates include 8–38 Tmol year^{-1} (Treguer et al. 1995),

25.5 Tmol year^{-1} (Laruelle et al. 2009) and 33–159 Tmol year^{-1} (Tréguer and De La Rocha 2013). Clearly, there is scope to improve these estimates. Here, I attempt this by using a compilation of porewater [Si] profiles from marine sediments to calculate diffusive Si fluxes out of sediment.

2 Methods

I compiled >450 published porewater [Si] records from the upper 40 cm of marine sediment cores (Fig. 1), assuming that the different methods of coring and sample collection yield comparable results. Most studies kept cores at in-situ temperatures to avoid chemical changes, though no attempt was made to identify and account for those that did not. Both theoretical and empirical studies have shown that porewater [Si] profiles can be described as an exponential function (e.g. McManus et al. 1995; Fig. 1):

$$[Si]_z = C_{asym} - (C_{asym} - C_0)e^{-\beta z} \tag{1}$$

where C_{asym} is an asymptotic concentration, C_0 is the overlying water concentration, β an exponential constant (cm^{-1}) and z the depth below sediment surface (cm). Values of C_{asym} and β were obtained for each profile by searching for the combination that minimised the RMSE between predicted and measured values. The 5% of poorest model fits were discarded. Differentiation of Eq. (1) at $z = 0$ provides the gradient across the sediment–water interface:

$$\left.\frac{d[Si]}{dz}\right|_{z=0} = \beta(C_{asym} - C_0) \tag{2}$$

which can then be used in Fick's first law to calculate the flux J (mol m^{-2} year^{-1}) across the sediment–water interface, assuming steady-state porewater DSi:

$$J = -\phi D \frac{d[Si]}{dz} \tag{3}$$

where D is dissolved Si diffusion coefficient which takes a value of ca. 0.03 m^2 year^{-1} at 25 °C (Wollast and Garrels 1971), and is corrected for sediment tortuosity and temperature after Boudreau (1996). In-situ temperature was extracted from the closest grid-cell of the WOCE ocean climatology (Gouretski and Koltermann 2004). A representative, uniform value of surface sediment porosity Φ (also required for the tortuosity correction) was prescribed at 0.9 for all sites. Finally, sediment lithology was identified at each location using the 0.1° resolution classification of Dutkiewicz et al. (2015).

3 Results and discussion

In total, 453 porewater profiles were compiled, of which 325 were at sufficiently high resolution to be included in the analysis. These data span the global ocean (Fig. 1B), though are biased towards the Atlantic. Calculated asymptote concentrations (C_{asym}) range from 9 to 862 µmol L^{-1}, and β values from 0.01 to 6 cm^{-1}. In all cases, the flux across the sediment–water interface was positive and ranges from 0.0017 to 3.35 mol m^{-2} year^{-1}, with mean = 0.22 and median = 0.10 mol m^{-2} year^{-1}. The fluxes are lognormally distributed, and are not systematically related to temperature, core depth or latitude (Fig. 2). Asymptote concentrations and exponential constants (β) are similarly unrelated to these parameters (data not shown).

Although the data is noisy, there are significant differences in diffusive fluxes from different sediment lithologies (Fig. 2A). Taking the area of these lithologies from the Dutkiewicz et al. (2015) digital map together with their diffusive fluxes (fitted to a lognormal distribution and using
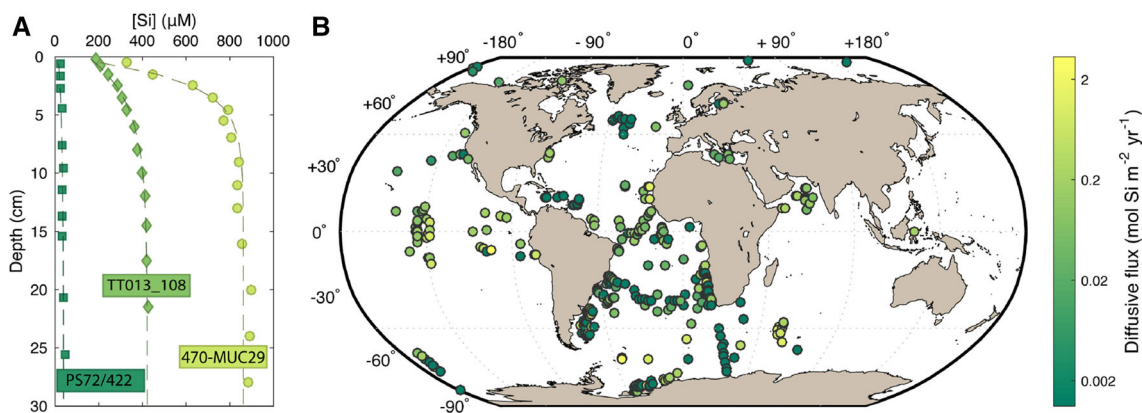

Fig. 1 Porewater [Si] profiles included in this analysis. **A** Typical [Si] profiles from the Arctic Ocean (core PS72/422, calculated flux = 0.0041 mol m^{-2} year^{-1}; März et al. 2015), the central Equatorial Pacific (core TT013_108, calculated flux = 0.080 mol m^{-2}-year^{-1}; McManus et al. 1995) and the Peruvian margin (core 470-MUC29, calculated flux = 0.68 mol m^{-2} year^{-1}; Ehlert et al. 2016). **B** The location of all cores with sufficient data to calculate a dissolved Si diffusive flux
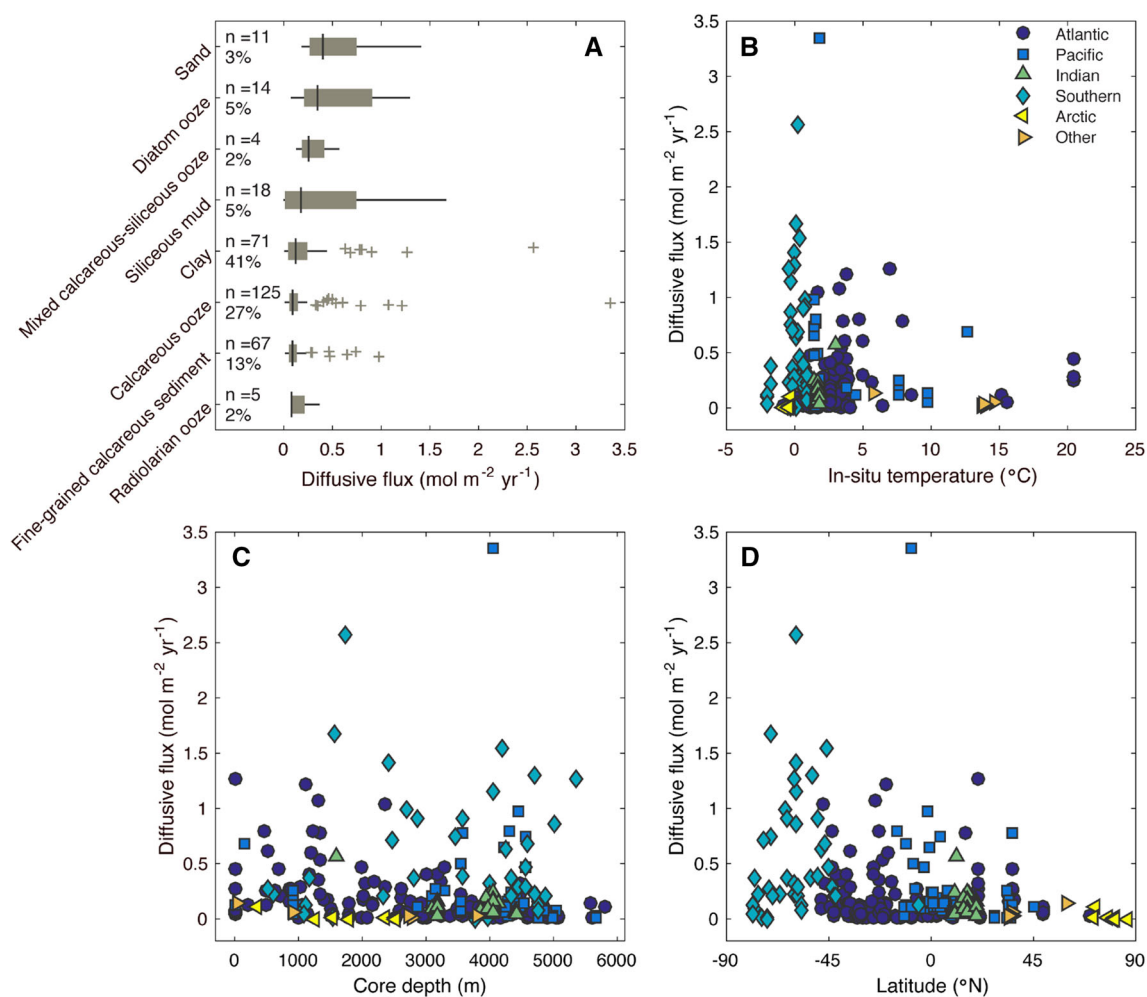
Fig. 2 Range of diffusive Si fluxes seen in the modern ocean. Fluxes vary significantly between sediment lithologies (**A**), but not with temperature (**B**), water depth (**C**) or latitude (**D**). Percentages in panel A indicate amount of ocean floor covered by each lithology

a Monte Carlo approach to uncertainty propagation) yields a median total flux of 69.5 Tmol year^{-1} (5th–95th percentiles: 64–232 Tmol year^{-1}), of which only 16.5 Tmol year^{-1} is from areas classified as siliceous (i.e. diatom, radiolarian or sponge oozes, or siliceous/siliceous-calcareous mud. The remainder (median = 44.9 Tmol year^{-1}) comes from clay or calcareous sediments, which together cover 284 × 10^6 km^2, or about 78% of ocean area (Dutkiewicz et al. 2015). This suggests regions not typically considered important in the ocean Si cycle may deserve more attention, simply because of their spatial extent. Tréguer and De La Rocha (2013) had previously considered diffusion from non-siliceous sediments to reflect dissolution/alteration of ocean basalts or terrigenous sediments. They employed an areal diffusive flux rate of 10–20 mmol m^{-2} year^{-1} from the study of Sayles et al. (1996), which is an order of magnitude less than the rate derived here for non-siliceous sediments. Either the dissolution of ocean basalt and terrigenous detrital

sediment is greatly underestimated in recent budgets, or there is a more active benthic biological Si cycle in these regions than conventionally recognised, perhaps via sponges (e.g. Alvarez et al. in review). A discrepancy also exists between the amount of bSi thought to arrive at the seafloor and that calculated to dissolve within the sediments. According to the sediment trap analysis of Honjo et al. (2008), 34.6 Tmol year^{-1} bSi sinks past 2 km. About 86% of ocean floor is below this depth, and given the lack of correlation between water depth and Si diffusive fluxes (Fig. 2C), then ca. 60 Tmol year^{-1} is calculated here to dissolve below this depth. This remains to be explained.

Assuming the marine Si cycle is close to steady-state, then ca. 9.5 × 10^{12} mol bSi year^{-1} is permanently buried (Frings et al. 2016), broadly consistent with independent estimates of bSi burial (e.g. DeMaster 2002). This implies a globally averaged sediment preservation efficiency of ca. 12%, in the same range as derived for individual regions

(see e.g. Ragueneau et al. 2009). This analysis confirms that a large fraction of bSi dissolution takes place in the sediment rather than the water column. The best estimate for the total dissolution flux is 69.5 Tmol year^{-1}, though the large associated uncertainties suggest it is rather more poorly understood than previously realised.

References

Alvarez B, Frings PJ, Clymans W, Fontorbe G, Conley DJ (in review) Assessing the potential of sponges (Porifera) as indicators of ocean dissolved Si concentrations. Front Mar Biogeochem

Boudreau BP (1996) The diffusive tortuosity of fine-grained unlithified sediments. Geochim Cosmochim Acta 60:3139–3142

DeMaster DJ (2002) The accumulation and cycling of biogenic silica in the Southern Ocean: revisiting the marine silica budget. Deep-Sea Res Part Ii-Top Stud Oceanogr 49:3155–3167

Dutkiewicz A, Müller RD, O'Callaghan S, Jónasson H (2015) Census of seafloor sediments in the world's ocean. Geology. doi:10.1130/g36883.1

Ehlert C, Doering K, Wallmann K, Scholz F, Sommer S, Grasse P, Geilert S, Frank M (2016) Stable silicon isotope signatures of marine pore waters—biogenic opal dissolution versus authigenic clay mineral formation. Geochim Cosmochim Acta 191:102–117

Frings PJ, Fontorbe G, Clymans W, De La Rocha CL, Conley DJ (2016) The continental Si cycle and its impact on the ocean Si isotope budget. Chem Geol 425:12–36

Gouretski V, Koltermann KP (2004) WOCE global hydrographic climatology. Berichte des BSH 35:1–52

Gunnarsson I, Arnórsson S (2000) Amorphous silica solubility and the thermodynamic properties of H_4SiO_4 in the range of 0 to 350 °C at P sat. Geochim Cosmochim Acta 64:2295–2307

Honjo S, Manganini SJ, Krishfield RA, Francois R (2008) Particulate organic carbon fluxes to the ocean interior and factors controlling the biological pump: a synthesis of global sediment trap programs since 1983. Prog Oceanogr 76:217–285

Laruelle GG, Roubeix V, Sferratore A, Brodherr B, Ciuffa D, Conley DJ, Dürr HH, Garnier J, Lancelot C, Le Thi Phuong Q, Meunier JD, Meybeck M, Michalopoulos P, Moriceau B, Ní Longphuirt S, Loucaides S, Papush L, Presti M, Ragueneau O, Regnier P, Saccone L, Slomp CP, Spiteri C, Van Cappellen P (2009) Anthropogenic perturbations of the silicon cycle at the global scale: key role of the land-ocean transition. Glob Biogeochem Cycles 23:GB4031

März C, Meinhardt AK, Schnetger B, Brumsack HJ (2015) Silica diagenesis and benthic fluxes in the Arctic Ocean. Mar Chem 171:1–9

McManus J, Hammond DE, Berelson WM, Kilgore TE, Demaster DJ, Ragueneau OG, Collier RW (1995) Early diagenesis of biogenic opal: dissolution rates, kinetics, and paleoceanographic implications. Deep Sea Res Part II 42:871–903

Ragueneau O, Regaudie-de-Gioux A, Moriceau B, Gallinari M, Vangriesheim A, Baurand F, Khripounoff A (2009) A benthic Si mass balance on the Congo margin: origin of the 4000 m DSi anomaly and implications for the transfer of Si from land to ocean. Deep Sea Res Part II 56:2197–2207

Sayles FL, Deuser WG, Goudreau JE, Dickinson WH, Jickells TD, King P (1996) The benthic cycle of biogenic opal at the Bermuda Atlantic Time Series site. Deep Sea Res Part I 43:383–409

Tréguer PJ, De La Rocha CL (2013) The world ocean silica cycle. Ann Rev Mar Sci 5:477–501

Treguer P, Nelson DM, Vanbennekom AJ, Demaster DJ, Leynaert A, Queguiner B (1995) The silica balance in the world ocean—a reestimate. Science 268:375–379

Wollast R, Garrels RM (1971) Diffusion coefficient of silica in seawater. Nature 229:94